Axially loaded Reinforced Masonry Walls under Cyclic Bending

(Elementi in muratura armata soggetti a carico assiale costante e momento flettente ciclicamente variabile)

E. CANTU'

Researcher, Istituto di Scienza e Tecnica delle Costruzioni, Università di Pavia - Italy

SUMMARY

Tests on plain and reinforced masonry elements were performed in order to determine interaction M-N diagrams.
Difficulties in the interpretation of the experimental values arose from the block failure mechanism strongly affected by a strain gradient effect.
The presence of vertical rebars favourably affected the behaviour under bending reversed cycles. The existence of "stabilized" conditions, characterized by a nonlinear elastic behaviour without appreciable energy dissipation, is of interest if seismic out-of-plane actions are taken into account.

SOMMARIO

Sono state effettuate prove sperimentali per determinare diagrammi d'interazione M-N per muratura semplice ed armata.

L'interpretazione dei risultati sperimentali è resa difficile dall'effetto del gradiente di deformazione sul meccanismo di rottura del blocco.

L'armatura verticale assicura un valido comportamento ciclico.

L'individuazione di condizioni "stabilizzate", caratterizzate da comportamento non lineare elastico, senza apprezzabile dissipazione d'energia, sembra particolarmente interessante in caso di azioni sismiche trasversali al piano degli elementi murari.

1. INTRODUCTION

A load-bearing wall in a structure generally undergoes in-plane and out-of-plane actions. Their effects are usually studied separately.

Here the behaviour of plain and reinforced masonry walls undergoing constant axial load and out-of-plane bending is described with particular interest in the observation of the strength variation under cyclic out-of-plane actions simulating the seismic effect on a wall in a structure.

The need of determining the complete axial load-bending moment interaction diagram is related to the variety of loading conditions that a wall can undergo in a real structure in case of earthquake.

The Reinforced Concrete theory is usually applied to reinforced masonry sections under bending and axial load [3] , but the accuracy of the theory depends on the kind of the masonry (coring percentage, coring pattern, ...)

2. SPECIMENS AND TEST SET-UP

2.1 Specimens

Dimensions and constituting materials were kept unchanged both in plain and reinforced specimens.

The 11 tested elements (5 plain and 6 reinforced) were 600 mm long, 175 mm thick and 1310 mm high; each wall was made of five courses of hollow units in running bond between upper and lower R.C. beams with a view of avoiding local failures in brickwork (Figure 1) and providing anchorage for steel bars. The masonry was made of hollow clay blocks and mortar having the following characteristics (Table 1).

The mechanical properties of masonry were determined by reference tests on small brickwork prisms (600x600x175 mm) under concentric axial load (Table 2).

The vertical reinforcement consisted of 2 deformed bars (Ø 8 mm). Bond between bars and blocks was assured by the surrounding mortar (Fig.1d). The characteristics of reinforcing steel are in Table 3.

2.2 Test set-up

The hinges at the top and bottom faces of the wall allow the application of the axial load N (Figs 2 and 3). The wall undergoes constant axial load and increasing imposed rotation at the bottom end. Figure 3 shows the loading condition. A load cell allowed to know the applied load F and a couple of transducers on each 600x1310 mm face made it possible to plot the eccentric load F versus mean compressive and tensile strains at the base of the wall.

TABLE 1 - Properties of materials

Units (hollow clay blocks) (Figure 1)	
nominal dimensions 290 x 175 x 190 (mm)	
coring 41%	
mean compressive strength (parallel to cores)	gross area = 32.3 N/mm^2
	net area = 49.1 N/mm^2
characteristic compressive strength (parallel to cores)	gross area = 27.2 N/mm^2
	net area = 41.3 N/mm^2
tensile splitting strength (net area)	= 3.2 N/mm^2
Cement mortar	
cement: lime: sand = 1:0:3 (by volume)	
mean compressive strength	= 12.1 N/mm^2
mean modulus of rupture	= 2.6 N/mm^2
modulus of elasticity	= 13400 N/mm^2

TABLE 2 - Properties of masonry

mean compressive strength (// to cores)	gross area 7.3 N/mm^2
	net area 11.1 N/mm^2
characteristic compressive strength (// to cores)	gross area 5.7 N/mm^2
	net area 8.7 N/mm^2
mean modulus of elasticity (// to cores)	E = 7600 N/mm^2

TABLE 3 - Properties of reinforcing steel

yielding strength	f_y = 393 N/mm^2
failure strength	f_r = 581 N/mm^2

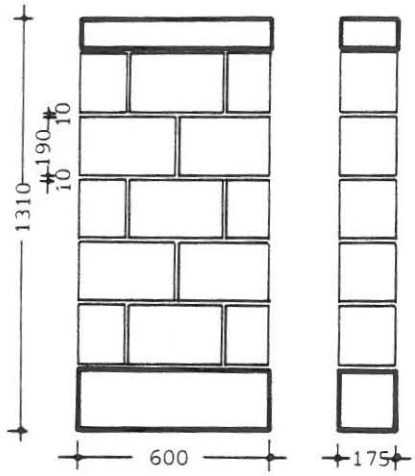

(a) plain masonry specimen

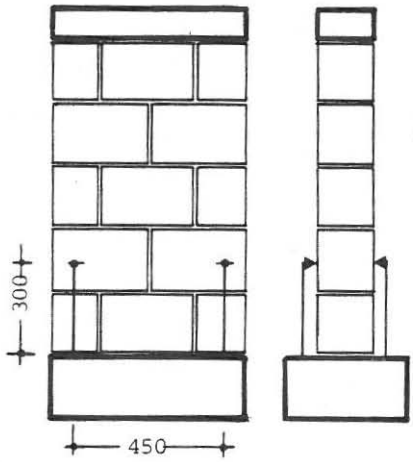

(b) gauge lengths for R.M. specimens

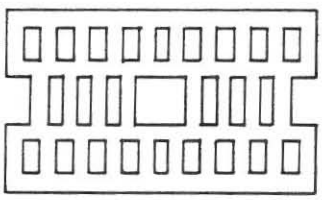

(c) block: coring pattern

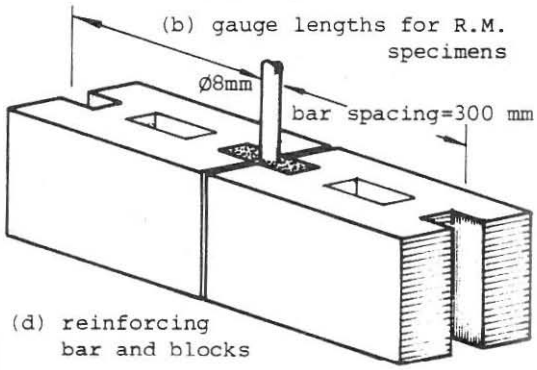

(d) reinforcing bar and blocks

FIGURE 1

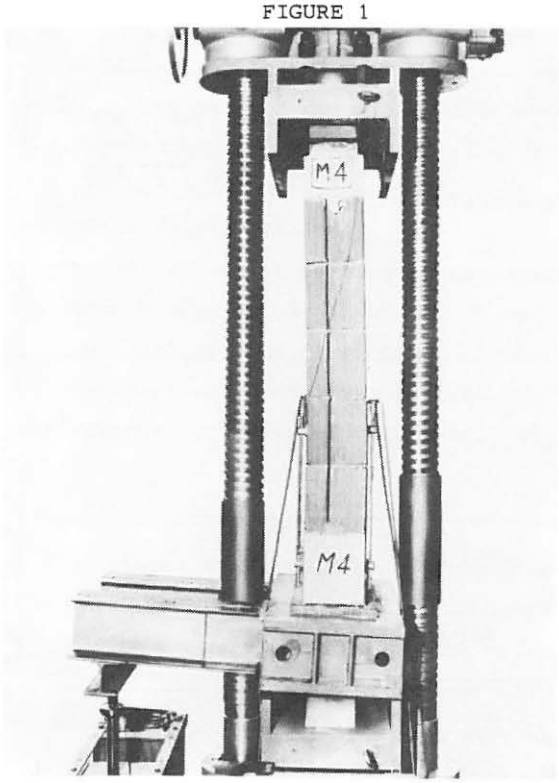

FIG. 2 - Testing equipment

FIG.3 - Loading condition for the tested elements.

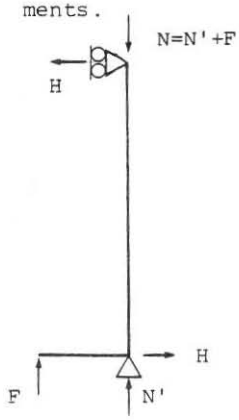

By imposing the rotation alternatively on either side of the wall, bending cycles were performed under nearly constant axial load.

3. INTERPRETATION OF EXPERIMENTAL RESULTS

3.1 Plain masonry

Walls undergoing eccentric load display apparent compression strength reserve when compared with axially loaded masonry.

The existence of this phenomenon was previously noticed |4,7| both for concrete blocks and clay bricks. The reasons can be found in the joined behaviour of units and mortar and specifically in the strain gradient effect.

The outstanding function of tensile strength of the units in determining the value of compressive strength of masonry in known |2| and is certainly higher in hollow block masonry, because of the reduction of transversal tensile strength due to perforation. Under eccentric loading the distribution of compressive stresses in the mortar induces a transversal tensile strain gradient in the units across the wall thickness. Consequently, the induced tensile stress field varies transversally as well.

In our case, the unit tensile strength can be imagined to vary with the extent of the stress field, similarly to what usually accepted for concrete prisms in bending: consequently the units in masonry under eccentric load can show an apparent higher tensile strength in the horizontal direction.

As above said, the tested masonry was made of hollow clay blocks: this could lead to further complexity in the interpretation of the experimental behaviour, due to the probable existence of more than one critical location in the unit |4|.

The above illustrated effect of the strain gradient on the bending strength is clearly evident if the experimental values are compared with a computed interaction diagram based on constant compression strength (Fig. 4). The curve was computed under the following hypotheses:

- linear strain diagram,
- rectangular stress block,
- net cross section,
- no longitudinal tensile strength,
- masonry compressive strength derived from compression tests and related to the net cross section (= 11.1 N/mm^2).

The observed failure modes are worth-while describing: they change with the $\frac{N}{N_u}$ ratio. In fact relatively high N values induce brittle failures on the compression side. The consequent reduction of the resisting cross section area

does not allow the wall to sustain the initial axial load.

On the contrary, relatively low N values do not lead to compression failure, but increase the wall flexural strength by prestressing the element, in such a way that even plain masonry specimens could undergo bending cycles.

In the latter situation the opening of cracks along horizontal bed mortar joints was evident as well as the progressive movement of the compressive resultant towards the outer clay layers of the blocks at the base of the specimen.

The different behaviour depending on the amount of the axial load could justify the assumption of a different value of compressive strength varying with the load eccentricity |7|.

Simple tests on couples of blocks were performed in order to clarify the above illustrated interpretation of the observed behaviour.

Similarly to previous tests performed by Amrein |1|, couples of blocks were loaded in uniform compression on an outer strip (varying in width from test to test) by means of rubber layers simulating the mortar joint effect. The performed tests allow to confirm a trend consistent with the hypothesis of compressive strength increasing with the load eccentricity, but the obtained values of compressive strength were not high enough to justify the experimental interaction diagram. (Neverthless, a more accurate choice of stiffness and size of the rubber layers could probably provide suitable results).

For practical applications, the interaction diagram computed under the usual assumptions and based on the compressive strength from compression tests on masonry prisms is on the safe side.

3.2 Reinforced masonry

As Fig.1d shows, the kind of examined reinforced masonry has reinforcing bars in holes and pockets of the blocks. The reinforcement is in the mid plane of the wall, so assuring a substantial entireness of the wall under cyclic actions.

The unchanged geometry of the two series of tested elements (plain and reinforced) allows the comparison of results: as foreseen, a relatively slight difference exists between the maximum bending values under the same axial load. Such difference tends to increase with increasing eccentricity.

3.3 Reinforced masonry under cyclic bending

The tests on 6 R.M. elements allow to represent the experimental results with more than 6 points in the M-N plane. This is a consequence of the adopted cyclic testing procedure and of the observed failure modes.

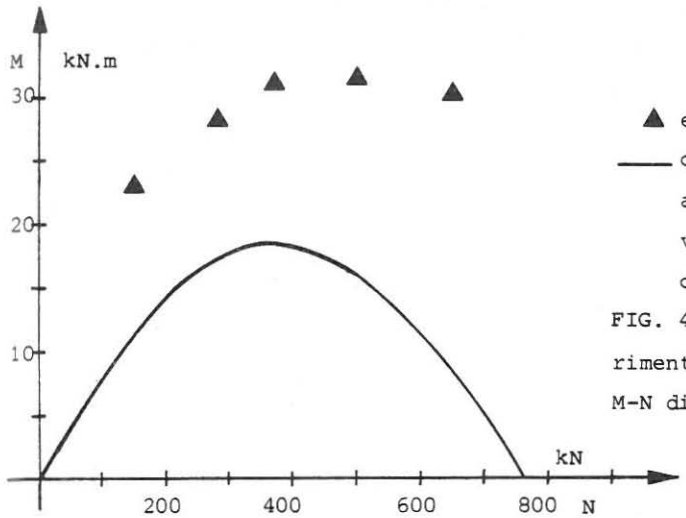

▲ experimental results

—— computed curve :net section and masonry strength as derived from compression tests on prisms

FIG. 4 - Comparison between experimental results and computed M-N diagram for the net section.

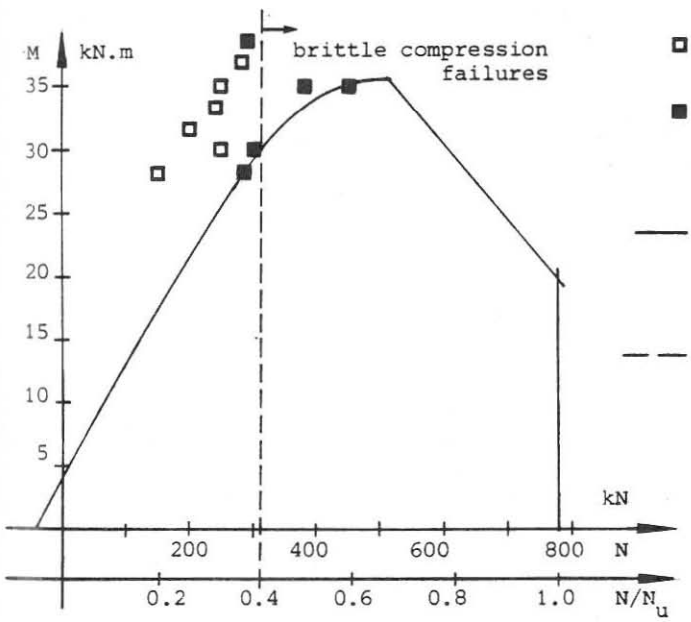

□ experimental points for R.M. specimens at 1st bending cycle;

■ experimental points for R.M. specimens, at 1st bending cycle, showing evident compression failures;

—— M-N diagram computed under the usual hypotheses of R.C. theory and assuming the fictitious masonry strength= 20 N/mm^2;

— — N/N_u limit value for brittle compression failures.

FIGURE 5 - Experimental points relating to the 1st performed cycles (tensile deformation limit = 2/300 mm/mm)

The failure behaviour depends again (as for plain masonry) on the value of the N/N_u ratio. Above a certain value of the axial load the compressive strength of the section is reached and a brittle failure suddenly reduces the section area: if the remaining area is likely to sustain the initial axial load, further cycles can be performed, attaining lower bending moments.

Under relatively low axial loads, the observed typical cyclic behaviour shows a decreasing degradation with decreasing axial load: at the lower limit, cycles can be repeated without any decrease in strength (Fig. 6).

A testing procedure was adopted according to the above illustrated observations: the specimens were first submitted to bending cycles under low N values, and subsequently to cycles under higher N values.

Five elements were tested under constant axial load and cyclic bending by imposing the same $\frac{2}{300}$ ($\frac{mm}{mm}$) ($=6.7 \times 10^{-3}$) deformation limit, that is mean strain on the tensioned side of the wall in the single half cycle (Fig. 1.b).

Under cycles having such imposed deformation, the value of the critical axial load inducing the beginning of sudden brittle failures was determined as to be about 40% of the load carrying capacity in concentric compression (Fig.5).

The 3 remaining elements, under the same deformation limit, were tested with axial load values higher than the above defined critical value. In particular, under the maximum examined N/N_u ratio, the observed brittle compression failure was of such importance that only a single cycle was performed (Fig. 7).

The N/N_u range between 0.40 and 0.60 is characterized by the possibility of sustaining loading cycles with evident degradation in strength and stiffness.

In order to study the effect of the amount of the imposed deformation, the 6th element underwent load cycles with gradually increasing axial load and mean strain limit of $\frac{4}{300}$ ($\frac{mm}{mm}$) ($= 13.3 \times 10^{-3}$), i.e. twice the deformation imposed in the previous tests.

The limit axial load value decreased ($N/N_u \simeq 0.30$) in comparison to the previous one ($N/N_u \cong 0.40$), due to the higher imposed rotation to the base of the wall.

4. FURTHER COMMENTS ON THE RESULTS

The previous considerations about the observed behaviour and the effect of the N/N_u ratio and the imposed limit deformations can be made clearer when referring to Figs 6 to 11.

Fig. 6 bears the experimental points corresponding to "stabilized" conditions: two kinds of points are shown due to the two values of the tensile deformation limit.

Consequently two interpolating curves were drawn: their maximum N values were

previously defined as $N = 0.40\ N_u$ and $N = 0.30\ N_u$ respectively. The two curves intersect due to the effect of the different deformation limits: under low N values, the higher limit deformation allows to reach higher bending moment values, the opposite is observed under relatively high N values.

Such behavioural characteristic is clarified in Figs 7 and 8: both related to a N/N_u ratio of $\simeq 0.25$ but under the two imposed deformation limits. The lower limit allows an evident stabilization, whereas the higher limit involves a certain amount of degradation before the stabilization can take place.

Fig. 9 refers to the lower deformation limit with $N/N_u = 0.40$, that is the limit value corresponding to brittle evident compression failures. In fact the strength and stiffness degradation is evident and, moreover, a sudden compression failure was observed when the deformation limit was slightly overstepped.

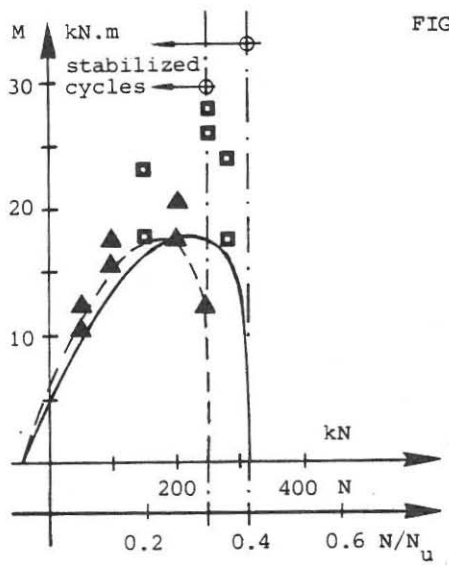

FIGURE 6 - Stabilized M-N diagrams

- ◘ experimental points representing "stabilized" conditions under the 2/300 mm/mm tensile deformation limit;
- ▲ as above but with 4/300 mm/mm tensile deformation limit;
- — "stabilized" M-N diagram with 2/300 mm/mm limit;
- – – "stabilized" M-N diagram with 4/300 mm/mm limit;
- —·— N/N_u limit values for both deformation limits.

In these conditions the failure shows the spalling of the most compressed outer clay layers in the blocks, as in Fig. 10.

At the limit, rather high N values preclude the possibility of performing cycles as Fig. 11 summarizes. Here the recorded diagrams were easily transformed in such a way as to bear bending moments versus rotations at the base of the wall. The test was performed with a N/N_u ratio of 0.60. During the 1st half cycle, a sudden failure in compression was observed, with large destruction of the compressive zone (Fig. 11.a). Nevertheless the remaining cross section area could undergo the same axial load and the reversed bending moment: the cycle

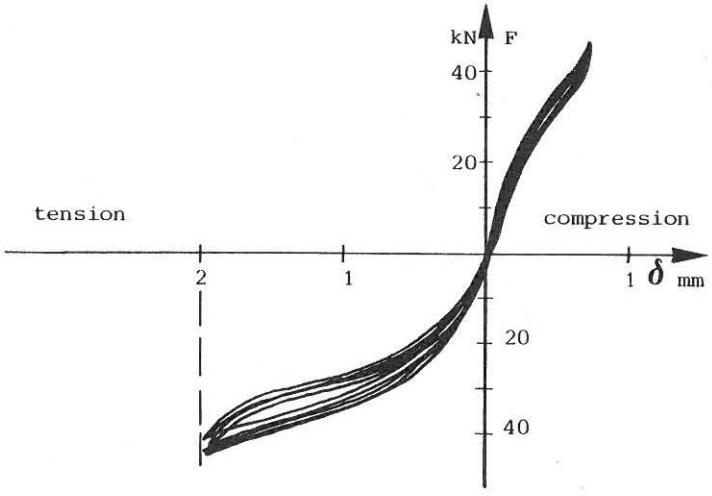

FIG. 7 - Typical"stabilized"cycles - N/N_u ratio =0.25 - Tensile deformation limit = 2/300 (mm/mm)

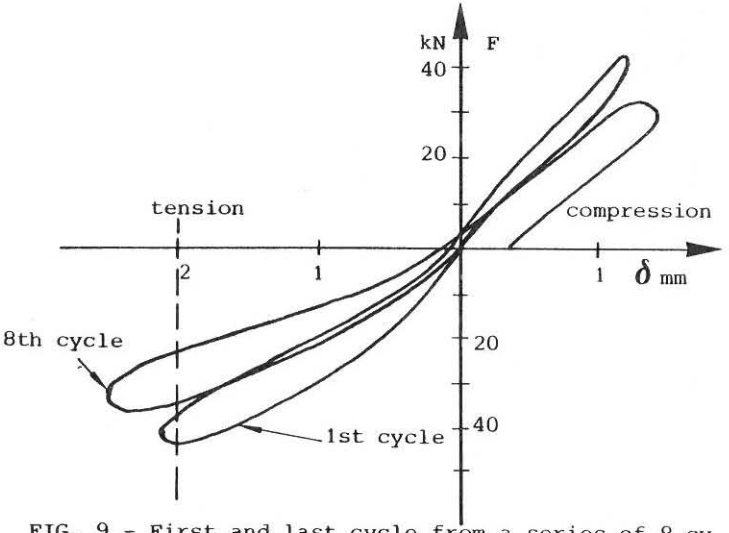

FIG. 9 - First and last cycle from a series of 8 cycles with tensile deformation limit of 2/300 mm/mm and N/N_u=0.4

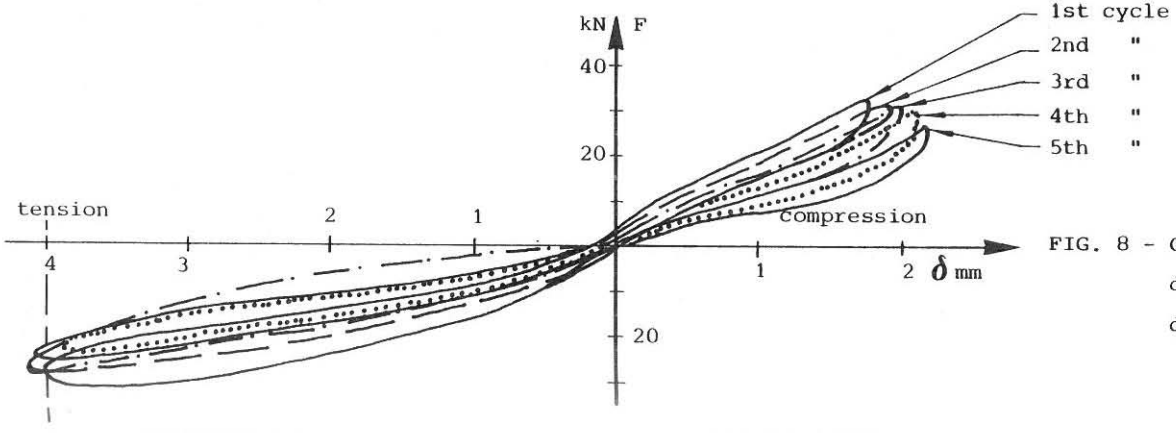

FIG. 8 - Cycles showing strength degradation- N/N_u=0.25 - Tensile deformation limit=4/300 mm/mm

was completed (Fig. 11.b) and again a compression failure was observed.

The unloading branches of the M-Ø curves in Fig. 11 were not recorded due to the detachment of the transducers in consequence of the compression failures.

5. CONCLUSIONS

The previous observations on the basis of the performed tests can be summarized as follows.

1. In monotonic loading, plain and reinforced masonry can be safely designed by assuming a rectangular stress block based on the masonry compressive strength derived from axial compression tests.
   Nevertheless, the wall actually shows a considerably higher bending strength, such increase being due to a strain gradient effect.
   The actual bending strength could be obtained by assuming a compressive strength value, varying with the eccentricity.

2. Further research is needed, in order to get a rational derivation of the strain gradient effect.

3. The reinforcement (of the examined kind and location) favourably affects the behaviour under cyclic out-of-plane loads. The definition of M-N domains corresponding to "stabilized" conditions under reversed cycles of M seems of particular interest under seismic actions perpendicular to the mean plane of the wall.

4. The "stabilized" interaction diagrams (within the M-N diagrams for the 1st cycle) vary with the compressive strength of masonry and with the imposed deformation. The limit axial load for a "stabilized" interaction diagram can be considered as to be that load causing evident,brittle compression failures, under the assumed deformation limit. Two tensile deformation limits were examined (2/300 mm/mm and 4/300 mm/mm), the above defined N/N_u limit values (signifying brittle failure) were 0.40 and 0.30 respectively.

5. In "stabilized" conditions the wall can be regarded as an assemblage of separate superimposed courses of blocks. The unloading and loading branches of the cycles are nearly superimposed: almost no energy dissipation takes place and the behaviour is nonlinear elastic. Ductility requirements can be fulfilled provided that no energy dissipation is demanded.

ACKNOWLEDGEMENT

The present work has been carried out with the grants of the National Research Council (C.N.R.) and of the A.N.D.I.L. (National Association of Brick Producers).

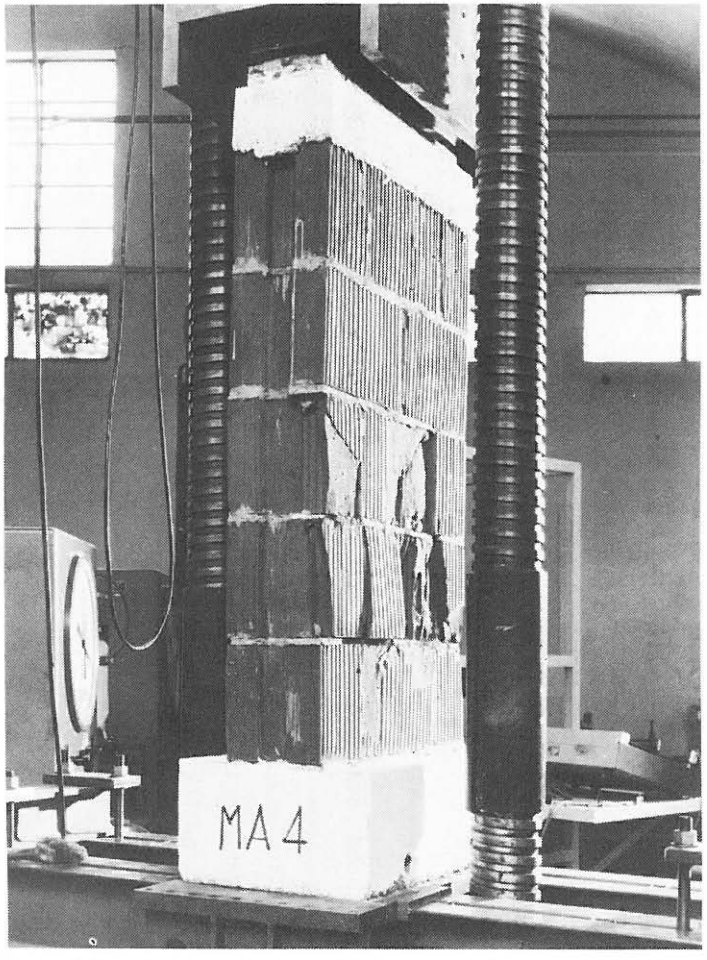

FIG. 10 - Compression failure with spalling of block outer clay layers

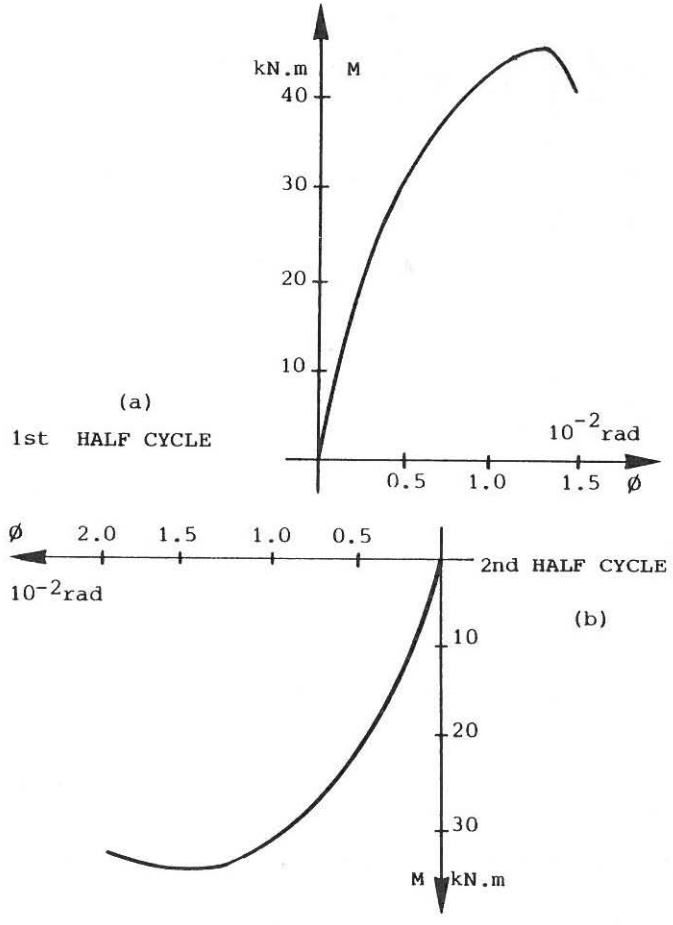

FIG. 11 - M-Ø diagrams for the specimen tested with N/N_u 0.60 and 2/300 mm/mm limit deformation (performed one cycle only)

6. REFERENCES

|1| Amrein E., Propriétés mécaniques des briques de provenance Suisse - Recherches et essais sur le structures en terre cuite. Colloque R.I.L.E.M. - Milan June, 25-28, 1962

|2| Hilsdorf H.K., Investigation into the Failure Mechanism of Brick Masonry Loaded in Axial Compression, Designing Engineering and Constructing with Masonry Products, Ed. by F.B. Johnson, Gulf Publishing Company, Houston, Texas, 1969

|3| The British Ceramic Research Association - Design Guide for Reinforced and Prestressed Clay Brickwork - Special Publication No. 91, 1977

|4| Turkstra, C.J., Thomas, G.R., Strain Gradient Effects in Masonry - Proceedings of the North American Masonry Conference, Boulder, Colorado, August 1978, Paper No. 22

|5| Zelger C.P., Tests on the Behaviour of the Compression Zone of Reinforced Masonry - Proc. of the British Ceramic Society, No. 27, Dec. 1978, Load-Bearing Brickwork (6)

|6| Furler R., Thürlimann B., Strength of Brick Walls under Enforced End Rotations - Proc. of the British Ceramic Society, No. 27, Dec. 1978, Load-Bearing Brickwork (6)

|7| Drysdale R.G., Hamid A.A., Effect of Eccentricity on the Compressive Strength of Brickwork, British Ceramic Society, Seventh International Load Bearing Brickwork Symposium, London, Nov. 1980

|8| Edgell G.J., Stress-Strain Relationships for Brickwork. Their Application in the Theory of Unreinforced Slender Members, British Ceramic Society, Seventh International Load Bearing Brickwork Symposium, London, 1980